

<https://doi.org/10.1038/s41525-024-00411-1>

Genomic analysis of 116 autism families strengthens known risk genes and highlights promising candidates

Check for updates

Marta Viggiano^{1,11}, Fabiola Ceroni^{1,2,11}, Paola Visconti³, Annio Posar^{3,4}, Maria Cristina Scaduto³, Laura Sandoni¹, Irene Baravelli¹, Cinzia Cameli¹, Magali J. Rochat⁵, Alessandra Maresca⁶, Alessandro Vaisfeld⁷, Davide Gentilini^{8,9}, Luciano Calzari⁹, Valerio Carelli^{4,6}, Michael C. Zody¹⁰, Elena Maestrini¹ ✉ & Elena Bacchelli¹ ✉

Autism spectrum disorder (ASD) is a complex neurodevelopmental condition with a strong genetic component in which rare variants contribute significantly to risk. We performed whole genome and/or exome sequencing (WGS and WES) and SNP-array analysis to identify both rare sequence and copy number variants (SNVs and CNVs) in 435 individuals from 116 ASD families. We identified 37 rare potentially damaging de novo SNVs (pdSNVs) in the cases ($n = 144$). Interestingly, two of them (one stop-gain and one missense variant) occurred in the same gene, *BRSK2*. Moreover, the identification of 8 severe de novo pdSNVs in genes not previously implicated in ASD (*AGPAT3*, *IRX5*, *MGAT5B*, *RAB8B*, *RAP1A*, *RASAL2*, *SLC9A1*, *YME1L1*) highlighted promising candidates. Potentially damaging CNVs (pdCNVs) provided support to the involvement of inherited variants in *PHF3*, *NEGR1*, *TIAM1* and *HOMER1* in neurodevelopmental disorders (NDD), although mostly acting as susceptibility factors with incomplete penetrance. Interpretation of identified pdSNVs/pdCNVs according to the ACMG guidelines led to a molecular diagnosis in 19/144 cases, although this figure represents a lower limit and is expected to increase thanks to further clarification of the role of likely pathogenic variants in ASD/NDD candidate genes not yet established. In conclusion, our study highlights promising ASD candidate genes and contributes to characterize the allelic diversity, mode of inheritance and phenotypic impact of de novo and inherited risk variants in ASD/NDD genes.

Autism spectrum disorder (ASD) is a neurodevelopmental condition characterized by social and communication difficulties, repetitive behaviours and unusually restricted or stereotyped interests¹. ASD is both clinically and genetically heterogeneous. Its architecture is characterized by a complex interplay between three major categories of genetic risk: common polygenic variation, rare inherited and de novo mutations. The contribution of each component varies between individuals. At one extreme, the susceptibility is mainly attributable to the

polygenic risk determined by thousands of common risk alleles, each exerting a small additive effect². At the other extreme, de novo variants (DNVs) can act as major contributors, leading in some cases to almost monogenic conditions. High-impact DNVs are estimated to affect at least 10% of ASD cases, but their contribution varies significantly according to the ascertainment strategy of the studied cohort, with a higher burden in ASD cases with comorbid intellectual disability (ID) and developmental disorders (DD)^{3–6}.

¹Department of Pharmacy and Biotechnology, University of Bologna, Bologna, Italy. ²Faculty of Health and Life Sciences, Oxford Brookes University, Oxford, UK. ³IRCCS Istituto delle Scienze Neurologiche di Bologna, UOSI Disturbi dello Spettro Autistico, Bologna, Italy. ⁴Department of Biomedical and Neuromotor Sciences, University of Bologna, Bologna, Italy. ⁵IRCCS Istituto delle Scienze Neurologiche di Bologna, Functional and Molecular Neuroimaging Unit, Bologna, Italy. ⁶IRCCS Istituto delle Scienze Neurologiche di Bologna, Programma di Neurogenetica, Bologna, Italy. ⁷Department of Medical and Surgical Sciences, University of Bologna, Bologna, Italy. ⁸Department of Brain and Behavioral Sciences, University of Pavia, Pavia, Italy. ⁹Bioinformatics and Statistical Genomic Unit, IRCCS Istituto Auxologico Italiano, Milan, Italy. ¹⁰New York Genome Center (NYGC), New York, NY, USA. ¹¹These authors contributed equally: Marta Viggiano, Fabiola Ceroni. ✉e-mail: elena.maestrini@unibo.it; elena.bacchelli@unibo.it

Given the large effect size of individual pathogenic DNVs, exome/genome sequencing studies (WES/WGS) of large cohorts of ASD families have led to a considerable progress in gene discovery, identifying hundreds of high-confidence genes involved in ASD or other neurodevelopmental disorders (NDDs) susceptibility^{4–6}.

The contribution of rare inherited variants has proven to be more difficult to be characterised. However, large family studies have recently managed to identify genes where the risk is mostly driven by rare loss-of-function (LoF) inherited variants, supporting the idea that by increasing the number of autism cases additional moderate-risk genes will be identified^{7,8}.

Early microarray studies have also significantly enhanced our understanding of the genetic landscape of ASD and other NDDs, pinpointing dozens of copy number variation (CNV) regions and dosage-sensitive genes^{9,10}. A recent study showed that 10.5% of NDD individuals carry CNVs of potential clinical relevance, of which about 40% are recurrent CNVs triggered by flanking repetitive sequences (recurrent genomic disorder, RGD), and >50% are CNVs disrupting one or more genes already implicated in NDDs¹¹. The overall resolution of CNV studies is now increasing thanks to WGS: this approach enables the discovery of previously undetected structural variations (small CNVs, CNVs in complex genomic regions and complex events), and strongly improves the ability to define the breakpoints, which is crucial for variant interpretation. WGS is thus standing out among less comprehensive technologies, as all sizes and types of variation are detectable with base-pair resolution in a single test⁶.

Despite these remarkable advances, many ASD cases remain genetically unexplained, highlighting a continuing need for further discovery efforts. In this context, family-based sequencing studies still represent a key approach for the identification of de novo variants with large effect that can provide new insights on risk genes, variant types and molecular mechanisms underlying the disorder, potentially offering promising targets for translational research.

Here, we present an integrated analysis of different classes of variants identified through WGS/WES and SNP-array in a cohort of 116 ASD multiplex and simplex families. This approach allowed us to characterize the contribution of rare de novo and inherited coding SNVs, indels and CNVs in our sample and to assess their phenotypic impact by exploring the presence of comorbidities in individuals carrying such variants.

Results

Overview of the cohort

Here we report the genomic characterisation of 435 individuals from 116 ASD families, comprising 144 individuals with ASD, 6 siblings with specific learning disabilities (SLD), 55 unaffected siblings, and 230 parents. Among the 144 affected individuals, 89 were from simplex families (SPX), 51 belonged to 25 multiplex families (MPX) and 4 to two monozygotic twin pairs. DNA samples were available for both parents for 114/116 families. Among the multiplex families, 22 included two affected siblings, one family included three affected siblings, while in two families the affected individuals were a child and a paternal uncle. The ASD individuals consisted of 110 males and 34 females, with a 3.2:1 male-to-female ratio.

Phenotypic data of ASD individuals, stratified by sex and family type (SPX/MPX), are reported in Supplementary Table 1. The mean age of symptoms onset was 15–16 months, with the majority of individuals (79%) presenting an early onset, and the mean age of diagnosis was 40 months (41.2 for males and 36.6 for females, two-sided *t*-test *p* value = 0.38) (Supplementary Fig. 1).

The mean ADOS-2 comparison score was 7.8 and the mean CARS2-ST was 39, with a significant difference between simplex and multiplex probands (two-sided *t*-test *p*-value ADOS-2 = 0.005, CARS2-ST = 0.001) (Supplementary Table 1 and Supplementary Fig. 2). The same trend was observed in the ICD-10 clinical diagnosis, where milder categories (F84.5 and F84.9) were more frequent among MPX probands (Fisher Exact test *p* value = 4.0×10^{-4}).

Mild to severe ID was present in 56% of probands, with 16/144 cases with severe ID, without a significant difference in cognitive levels between male and female probands and SPX and MPX. The vast majority of

probands had language problems (98.6%) and the rate of females with absent speech was significantly higher than in males (16/34 vs 30/110, χ^2 *p* value = 0.03). Only 12 probands presented epilepsy (8%). EEG and MRI anomalies were identified in 30/126 and 36/124 individuals, respectively, with no significant differences among groups (Supplementary Table 1). Analysis of MRI data of this cohort has been previously described¹².

The score distribution of Social and Communication Disorders Checklist (SCDC)¹³ in the entire cohort and of The Broad Autism Phenotype Questionnaire (BAPQ)¹⁴ in parents are shown in Supplementary Fig. 3. There are no significant differences in BAPQ scores between SPX and MPX or between parents of male-only or female-containing families (Supplementary Table 2a); 7 mothers (6 SPX and 1 MPX) and 4 fathers (6 SPX and 1 MPX) were above the threshold. Similarly, the mean SCDC values of ASD individuals, parents and unaffected siblings do not differ between sex or family type (Supplementary Table 2b).

Genetic data consisted of Illumina Infinium PsychArray genotyping for all families, WGS of 105 families and WES of 29 families (Supplementary Fig. 4).

MDS analysis was performed for ancestry determination, anchoring our cohort data to the 1000 Genomes Project. We visually inspected the first two MDS coordinates and found no discrepancy between genotype-computed and self-reported ancestry. Individuals of non-European ancestry comprise ~15% of our sample (66 individuals from 19 families, for a total of 26 cases), including one African, one South Asian and 17 Admixed families (Supplementary Fig. 5).

Rare coding sequence variant analysis

We analysed WES and WGS data from all 435 individuals of our cohort, focussing on rare variants affecting coding exons and canonical splice sites as these provide the most direct links between gene function and disease pathogenesis. We did not use WGS data to investigate mitochondrial DNA, as deep sequencing of the entire mitogenome and quantification of mtDNA cellular content of this cohort has been previously described¹⁵.

We identified a total of 243 rare DNVs in protein-coding exons (MAF \leq 0.1% in reference databases): 178 in 144 ASD individuals and 65 in 55 unaffected siblings (Fig. 1a).

The number of DNVs per child was consistent with the rate reported in other studies⁴ and similar between individuals with autism and their siblings (mean rate of 1.24 and 1.18, respectively). The percentage of cases and unaffected siblings carrying at least one rare de novo SNV (cases: 103/144, 71.5%; unaffected siblings: 35/55, 63%; χ^2 *p* value = 0.28) was also comparable to previous studies.

We catalogued rare DNVs in six bins of predicted functional severity: two bins for PTVs according to the LOEUF score¹⁶, three bins for missense variants based on the MPC score¹⁷, and a single bin for synonymous variants. The variants predicted to be more deleterious account for 24% of the DNVs found in cases: 5.1% were PTVs in constrained genes (LOEUF < 0.6), hereafter referred to as “PTV_{LOEUF}”, and 18.2% were damaging missense variants with MPC \geq 1 (Dmis), among which 6.9% with MPC \geq 2 (DmisB) and 11.3% with $1 \leq$ MPC < 2 (DmisA). The remaining DNVs were missense with MPC < 1 (43%), synonymous (26%), and PTVs in unconstrained genes (7%), consistently with the previously reported bin distribution in a family sample of 6,430 ASD cases⁴. Interestingly, no PTV_{LOEUF} were identified in unaffected siblings, supporting a larger effect on the liability of this class of variants (Fig. 1b, Supplementary Table 3).

Among the 37 rare de novo PTV_{LOEUF} and Dmis identified in our cases, hereafter defined as potentially damaging SNVs (pdSNVs), two (one PTV and one DmisB) occurred in *BRSK2* in two different families (Table 1). Beyond these de novo pdSNVs, we also identified a stop-gain variant of unknown origin in *SHANK3* in the female proband of simplex family 123 (maternal DNA was unavailable). However, since LoF variants in *SHANK3* usually arise de novo⁸, this was deemed as likely de novo (Table 1). To further assess the potential relevance of these 38 pdSNVs, we used the LOFTEE¹⁶, pext¹⁸ and AlphaMissense¹⁹ annotations (Supplementary Table 4). All 9 PTVs were high-confidence LoF variants according to LOFTEE and

occurred in brain-expressed exons. Specifically, 7 involved bases constitutively expressed in the brain (pext score >0.9), while two (the frameshift variants in *URB5* and *BRSK2*) fell in exons with an intermediate expression in the brain (0.46 and 0.69, respectively). However, the exon containing the *BRSK2* variant showed a much higher expression in the brain compared to the mean aggregate expression, including all tissues (0.69 vs 0.1). Among the 11 DmisB, all but one (*MGAT3* p.T468M) were predicted “likely_pathogenic” by AlphaMissense ($LP_{\alpha M}$) and all involved brain-expressed exons. Among the 18 DmisA, 9 were $LP_{\alpha M}$ and all occurred in brain-expressed exons.

STRING enrichment analysis of the 36 genes hosting the 38 de novo pdSNVs in probands detected a significant enrichment in gene interactions

(12 vs 5 expected edges, 2.4-fold enrichment, p value = 0.00318, one-tailed hypergeometric test), whereas no significant interaction enrichment was identified for 40 genes hosting 42 synonymous de novo variants in probands (4 vs 3 expected edges, p -value = 0.456), nor for 12 genes hosting the 13 de novo pdSNVs (4 DmisB and 9 DmisA) identified in unaffected siblings (0 vs 0 expected edges, p value = 1).

When we restricted the STRING analysis to the 17 genes hosting the 19 most severe de novo pdSNVs (9 high-confidence PTV_{LOEUF} and 10 DmisB $LP_{\alpha M}$), there was still a significant interaction enrichment (4 vs 1 expected edges, p value = 0.0389). Gene Ontology (GO) enrichment analysis of these 17 genes identified 10 genes in the “regulation of transport” category (GO:0051049, 6.48-fold enrichment, $FDR = 3.88 \times 10^{-3}$), and in the

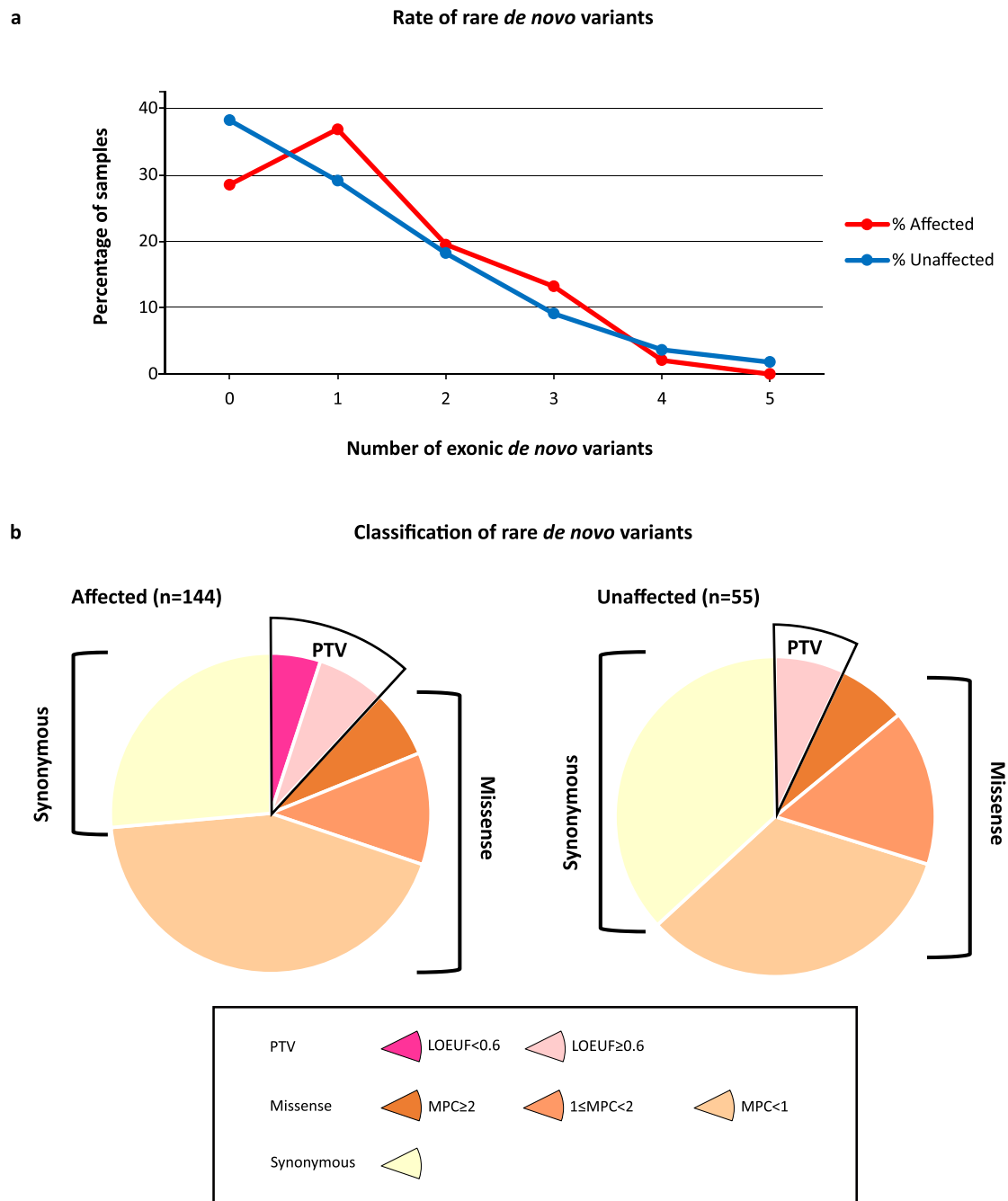


Fig. 1 | Rare de novo coding variants in cases and unaffected siblings. **a** Rare coding de novo variants per individual in our cohort (ASD cases=144, unaffected siblings=55). **b** Distribution of rare de novo coding variants in cases and unaffected siblings: the pie charts represent rare de novo coding variants split by predicted

functional consequences, represented by different colours. PTVs and missense variants are divided into two and three tiers of predicted functional severity, represented by different shade, based on the LOEUF (<0.6, ≥0.6) and MPC metrics (MPC ≥ 2 (DmisB), 1 ≤ MPC < 2 (DmisA), 0 ≤ MPC < 1), respectively.

Table 1 | List of de novo pdSNVs identified in affected individuals

Variant location ^a	ACMG class ^b	Individual (Family structure) ^c	Symptoms Onset Pattern; ADOS-2 (Diagnosis, comparison score); CARS2-ST score; Language level; ID level (test, score); Epilepsy ^d
a) PTV_{LOEUF}			
NM_002884.4(RAP1A): c.73 C > T (p.Q25X)	P (PVS1,PS2,PM2,PP3)	69.3 (f/m/aM)	EO; ADOS-2 (Autism, 9); CARS2-ST: 41.5; Absent speech; Moderate ID (NA); Focal epilepsy
NM_170692.4(RASAL2): c.2560 C > T (p.Q854X)	LP (PS2,PM2,PP3)	19.3 (f/m/aM)	EO; ADOS-2 (Autism, 6); CARS2-ST: 42.5; Absent speech; Mild ID (NA)
NM_006922.4(SCN3A): c.4888 C > T (p.R1630X)	LP (PS2,PM2,PP3,BS4)	40.3 (f/m/aM/aM)	Mixed; ADOS-2 (Autism, 9); CARS2-ST: 37.5; Single words; Normal IQ (Leiter-R, B-IQ 117, FR 108)
NM_001040142.2(SCN2A): c.4180 C > T (p.Q1394X)	P (PVS1,PS2,PM2,PP3,BS4)	113.4 (f/m/aF/raM/uF)	EO; ADOS-2 (Autism, 10); CARS2-ST: 43; Absent speech; Severe ID (NA)
NM_015902.6(UBR5): c.7441del (p.H2481Mfs*7)	LP (PVS1,PS2,PM2,BS4)	110.3 (f/m/aM/aM/uMs)	EO; ADOS-2 (Autism, 6); CARS2-ST: 37; Atypical language; Borderline IQ (Leiter-R, B-IQ 74)
NM_001256627.2(BRSK2): c.1620_1621del (p.D540Efs*9)	P (PVS1,PS2,PM2)	32.3 (f/m/aM/uM)	EO; ADOS-2 (Autism, 6); CARS2-ST: 39.5; Single words; Normal IQ (Leiter-R, B-IQ 96, FR 108)
NM_005853.6(IRX5): c.28 C > T (p.Q10X)	P (PVS1,PS2,PM2,PP3)	102.3 (f/m/aM)	EO; ADOS-2 (Autism, 10); CARS2-ST: 39; Atypical language; Borderline IQ (NA)
NM_001372044.2(SHANK3): c.2611 G > T (p.E871X)	P (PVS1,PM2,PM6, PP3)	123.3 (f/aF) ^e	EO; ADOS-2 (Autism, 9); CARS2-ST: 43.5; Absent speech; Severe ID (NA)
NM_001372044.2(SHANK3): c.4871 C > A (p.S1624X)	LP (PS2,PM2,PP3)	29.3 (f/m/aF/uM)	EO; ADOS-2 (Autism, 8); CARS2-ST: 43; Absent speech; Profound ID (GMDS 0-2, CA 11 y, total AE 12,75 m); Focal epilepsy
b) DmisB			
NM_003047.5(SLC9A1): c.1172 A > G (p.E391G)	LP (PS2,PM1,PM2,PP2)	98.3 (f/m/aM)	EO; ADOS-2 (Autism, 10); CARS2-ST: 42; Single words; Borderline IQ (Leiter-R, B-IQ 76, FR 84)
NM_014263.4(YME1L1): c.1981G>A (p.E661K)	LP (PS2,PM1,PM2,PP3,BS4)	117.3 (f/m/aM/aF)	EO; ADOS-2 (Autism, 9); CARS2-ST: 35.5; Atypical language; Mild ID (WPPSI-III, V-IQ 80, P-IQ 65, Total IQ 66); Focal epilepsy
NM_001256627.2(BRSK2): c.472 G > A (p.A158T)	LP (PS2,PM1,PM2,BS4)	14.4 (f/m/aM/aM)	EO; ADOS-2 (Autism, 8); CARS2-ST: 39; Absent speech; Moderate ID (NA)
NM_002804.5(PSMC3): c.1180 G > A (p.A394T)	LP (PS2,PM1,PM2,PP3)	106.3 (f/m/aM)	EO; ADOS-2 (Autism, 9); CARS2-ST: 42.5; Absent speech; Severe ID (NA)
NM_001376.5(DYNC1H1): c.7501 T > C (p.S2501P)	LP (PS2,PM2)	122.3 (f/m/aM)	EO; ADOS-2 (Autism, 9); CARS2-ST: 36; Single words; Normal IQ (NA)
NM_016530.3(RAB8B): c.227 C > T (p.A76V) ^f	LP (PS2,PM1,PM2,PP3,BS4)	85.3 (f/m/aM/aM)	Mixed; ADOS-2 (Autism, 7); CARS2-ST: 45; Absent speech; Moderate ID (NA)
NM_001199172.2(MGAT5B): c.1177 G > A (p.D393N) ^f	LP (PS2,PM1,PM2,PP3,BS4)	15.3 (f/m/aM/aM)	EO; ADOS-2 (Autism, 9); CARS2-ST: 42.5; Single words; Normal IQ (Leiter-R, B-IQ 89, FR 84)
NM_004218.4(RAB11B): c.98 G > A (p.R33H)	LP (PS2,PM1,PM2,PP2)	52.3 (f/m/aM)	EO; ADOS-2 (Autism, 6); CARS2-ST: 39; Single words; Mild ID (Leiter-R, B-IQ 56, FR 63); Focal epilepsy
NM_001365902.3(NFIX): c.224 T > C (p.L75P)	LP (PS2,PM1,PM2,PP3,BP1)	81.3 (f/m/aM/uM)	EO; ADOS-2 (Autism, 10); CARS2-ST: 39.5; Absent speech; Severe ID (GMDS 0-2, CA 34 m, total AE 10 m)
NM_020132.5(AGPAT3): c.536 G > A (p.R179H)	LP (PS2,PM1,PM2,PP3)	17.3 (f/m/aM/uM)	Regressive; ADOS-2 (Autism, 9); CARS2-ST: 37; Single words; Mild ID (Leiter-R, Full IQ 57, FR 48)
NM_002409.5(MGAT3): c.1403 C > T (p.T468M) ^f	LP (PS2,PM2)	5.3 (f/m/aM)	EO; ADOS-2 (Autism, 5); CARS2-ST: 39.5; Single words; Borderline IQ (Leiter-R, B-IQ 79, FR 62)
c) DmisA			
NM_152365.3(KDF1): c.1058 C > T (p.S353F)	LP (PS2,PM2,PP2)	81.3 (f/m/aM/uM)	EO; ADOS-2 (Autism, 10); CARS2-ST: 39.5; Absent speech; Severe ID (GMDS 0-2, CA 34 m, total AE 10 m)
NM_138417.3(KTI12): c.176 G > A (p.R59H)	LP (PS2,PM2,PP3,BS4)	16.4 (f/m/aM/aM)	EO; ADOS-2 (Autism, 9); CARS2-ST: 39; Absent speech; Moderate ID (PEP-3, CA 2.7 y, cognitive-verbal AE < 12 m)
NM_001348768.2(HECW2): c.2426 T > C (p.L809P)	P (PS2,PM1,PM2,PP2,PP3)	68.3 (f/m/aF/uF/uM)	Mixed; ADOS-2 (Autism, 10); CARS2-ST: 38.5; Absent speech; Borderline IQ (Leiter-R, B-IQ 74, FR 73)
NM_152783.5(D2HGDH): c.376 G > A (p.V126M) ^f	LP (PS2,PM1,PM2,PP3)	87.3 (f/m/aM/uM)	EO; ADOS-2 (Autism, 6); CARS2-ST: 40.5; Single words; Mild ID (Bayley-III, CA 38 m, AE 19 m)
NM_001967.4(EIF4A2): c.727 A > G (p.T243A)	LP (PS2,PM1,PM2,BS4)	110.4 (f/m/aM/aM/uMs)	EO; ADOS-2 (ASD, 4); CARS2-ST: 33; Atypical language; Normal IQ (Leiter-R, B-IQ 107, FR 102)
NM_001010852.4(CLVS2): c.142 C > G (p.R48G)	LP (PS2,PM1,PM2)	44.3 (f/m/aM/uF)	EO; ADOS-2 (Autism, 7); CARS2-ST: 45; Single words; Mild ID (Leiter-R, B-IQ 54, FR 52)
NM_000368.5(TSC1): c.2023 G > T (p.D675Y)	LP (PS2,PM1,PM2,PP3)	100.3 (f/m/aF)	EO; ADOS-2 (Autism, 9); CARS2-ST: 40; Single words; Mild ID (NA)

Table 1 (continued) | List of de novo pdSNVs identified in affected individuals

Variant location ^a	ACMG class ^b	Individual (Family structure) ^c	Symptoms Onset Pattern; ADOS-2 (Diagnosis, comparison score); CARS2-ST score; Language level; ID level (test, score); Epilepsy ^d
NM_182765.6(HECTD2): c.742 G > A (p.V248I)	LP (PS2,PM1,PM2)	30.3 (f/m/aM/uM)	EO; ADOS-2 (Autism, 9); CARS2-ST: 41.5; Absent speech; Moderate ID (PEP-3, CA 3 y, cognitive-verbal AE 17 m)
NM_020123.4(TM9SF3): c.941 T > C (p.I314T)	LP (PS2,PM2,BS4)	12.5 (f/m/aM/uM/aM)	EO; ADOS-2 (Autism, 6); CARS2-ST: 33.5; Single words; Mild ID (GMDS 0-2, CA 17 m, total AE 11 m)
NM_032138.7(KBTBD7): c.1849C>T (p.R617C)^f	VUS (PS2,PP3,BS4)	40.4 (f/m/aM/aM)	Mixed; ADOS-2 (Autism, 8); CARS2-ST: 34.5; Atypical language; Normal IQ (Leiter-R, B-IQ 111, FR 88)
NM_021239.3(RBM25): c.1052 G > A (p.R351H) ^f	LP (PS2,PM1,PM2)	60.3 (f/m/aF)	EO; ADOS-2 (Autism, 10); CARS2-ST: 48; Single words; Moderate ID (PEP-3, CA 5.6 y, cognitive-verbal AE 36 m)
NM_001017919.2(RCCD1): c.419 C > A (p.A140D)	VUS (PS2,PM1,PM2,BS4,BP4)	117.4 (f/m/aM/aF)	EO; ADOS-2 (Autism, 8); CARS2-ST: 34.5; Single words; Normal IQ (Leiter-3, IQ 97)
NM_000430.4(PFAFH1B1): c.431 G > A (p.R144Q)	LP (PS2,PM1,PM2,BS4)	15.4 (f/m/aM/aM)	EO; ADOS-2 (Autism, 6); CARS2-ST: 33; Normal language; Borderline IQ (WISC-IV, Full IQ 78)
NM_032442.3(NEURL4): c.2170 G > A (p.G724S) ^f	LP (PS2,PM1,PM2,PP3,BS4)	115.3 (f/m/aF/aM/aF)	EO; ADOS-2 (Autism, 6); CARS2-ST: 36; Single words; Moderate ID (GMDS, CA 27 m, total AE 5.5 m)
NM_014738.6(TMEMP94): c.3202 C > T (p.R1068C) ^f	LP (PS2,PM1,BP1)	101.3 (f/m/aM)	EO; ADOS-2 (ASD, 4); CARS2-ST: 36.5; Absent speech; Moderate ID (GMDS, CA 43 m, total AE 21.5 m)
NM_017534.6(MYH2): c.3458 G > A (p.S1153N)	LP (PS2,PM1,PM2,PP3,BS4)	77.3 (f/m/aM/aF/uM/uFs)	EO; ADOS-2 (Autism, 9); CARS2-ST: 41.5; Single words; Mild ID (Leiter-R, NA)
NM_007050.6(PTPRT): c.1076 G > A (p.R359Q) ^f	LP (PS2,PM1)	72.3 (f/m/aF/uF)	EO; ADOS-2 (Autism, 6); CARS2-ST: 34; Single words; Mild ID (Leiter-R, NA)
NM_017436.7(A4GALT): c.562 G > A (p.G188S) ^f	LP (PS2,PM1,PM2,PP3)	90.3 (f/m/aF/dM)	EO; ADOS-2 (Autism, 9); CARS2-ST: 41; Absent speech; Moderate ID (PEP-3, CA 4 y, cognitive-verbal AE 24 m)

De novo pdSNVs include PTVs in genes with LOEUF score <0.6 (PTV_{LOEUF}), missense variants with MPC ≥ 2 (DmisB) and missense variants with 1 ≤ MPC < 2 (DmisA). All reported variants are novel considering the non-neurological subset of gnomAD v.2.1.1 and v.3.1.2, except for variants labelled with ^f. ^aAmino acid changes are reported according to the MANE isoform; Variant in high-confidence ASD/NDD gene list classification according to Table S8 are indicated in bold; ^bClassification of genetic variants according to the ACMG guidelines, together with detailed evidence codes, was performed using InterVar. *P* pathogenic, *LP* likely pathogenic, *VUS* variant of uncertain significance, ^cProbands are indicated with an identifier code formed by the family number and the individual number. In brackets, the family structure is reported with children listed sequentially after the father and the mother, according to the recruitment order. The affected individual heterozygote for the variant is underlined. *f* father, *m* mother, *r* relative (uncle), *s* half-sib, *a* affected, *u* unaffected, *M* male, *F* female. ^dEpilepsy is present only where it is explicitly indicated. *EO*, Early Onset, *NA* Not Assessed, *V-IQ* Verbal IQ, *P-IQ* Performance IQ, *B-IQ* Brief IQ, *FR* Fluid Reasoning, *CA* chronological age, *AE* age equivalent, *GMDS* Griffiths Mental Development Scales, *m*, months, *y* years. ^eSince DNA of the biological mother was unavailable, de novo status was only assumed. ^fRare variant, present in gnomAD v.2.1.1 and v.3.1.2 “non-neuro” dataset with MAF ≤ 0.01%.

“regulation of localization” category (GO:0032879, 5.7-fold enrichment, FDR = 1.07 × 10⁻²), while no biological process resulted to be enriched for the 40 genes with de novo synonymous variants (Supplementary Table 5).

We next assessed the rate of de novo and inherited pdSNVs in cases and unaffected siblings and found no overall excess of such variants in cases (Supplementary Fig. 6).

Then, we tested if there was a difference in paternal and maternal origin of inherited pdSNVs in ASD individuals, but we did not identify any bias in transmission considering all pdSNVs (1300 paternal vs 1259 maternal), novel pdSNVs only (401 paternal vs 411 maternal), or only novel pdSNVs not shared with unaffected sibs (315 paternal vs 309 maternal).

Given the well-known role of synaptic genes in ASD pathogenesis, we used the SynGO platform²⁰ (dataset version: 20210225) to investigate whether the affected individuals showed an enrichment of rare pdSNVs in genes involved in synaptic components or functions. Among the 2,156 genes harbouring pdSNVs in cases (Supplementary Table 6), 254 were SynGO annotated genes. When compared with the “brain expressed” background set (18,035 unique genes including 1,225 SynGO annotated genes), our list showed a significant enrichment at 1% FDR for 13 Cellular Component (CC) terms and 5 Biological Processes (BP) terms (Fig. 2, Supplementary Table 7a). A similar pattern was obtained when we restricted the enrichment analysis to the category of novel pdSNVs or novel pdSNVs not shared with unaffected siblings: a significant enrichment at 1% FDR was retained for about the same number of GO terms (Supplementary Fig. 7, Supplementary Table 7b-c), maintaining the same four most significant CC and BP terms (synapse, process in the synapse, post-synapse, synapse organization). In contrast, the same analysis performed on the 6,666 genes carrying rare synonymous variants in ASD individuals highlighted 517 SynGO annotated genes, without any significant enrichment for CC or BP terms (Fig. 2).

To assess the contribution of deleterious variants in high-confidence ASD and/or NDD genes (*n* = 684, Supplementary Table 8)^{5,6}, we selected all the de novo/inherited pdSNVs located in such genes in ASD individuals and unaffected siblings. Our study identified rare pdSNVs in 97/232 high-confidence ASD genes (Fig. 3a) and in 139/452 high-confidence NDD genes (Fig. 3b). When we restricted the selection only to novel pdSNVs, we found that these pdSNVs affected 46 ASD genes (Supplementary Fig. 8a) and 64 NDD genes (Supplementary Fig. 8b).

While the rate of inherited rare variants in the 684 ASD/NDD genes was similar between cases and unaffected siblings, we observed an increased rate of de novo variants in ASD/NDD genes in affected individuals (16/144 cases (11.1%) vs 1/55 unaffected sibs (1.8%), Fisher’s exact test *p*-value = 0.04). Interestingly, probands carrying de novo pdSNVs in these genes versus those who did not, showed a significant positive association with severe ID (nonverbal IQ < 35) (Fisher’s Exact test *p* value = 0.018, OR = 4.83) (Supplementary Table 9a). When considering only the most severe de novo/inherited pdSNVs (16 high-confidence PTV_{LOEUF} and 37 DmisB LP_{aM}), 49 cases (34%) had at least one variant in these genes (3 probands had 2 severe pdSNVs). Comparing the probands with and without severe pdSNVs, we observed a significant association with severe ID (Fisher’s Exact test *p* value = 0.022, OR = 3.8) (Supplementary Table 9a). Significant associations were retained when restricting the analysis to novel de novo pdSNVs, and to novel severe pdSNVs (Fisher’s Exact test *p* value = 0.014 and 0.021, respectively) (Supplementary Table 9b).

Rare copy number variant analysis

Discovery of rare CNVs was performed by integrating CNV calls from SNP-array data on the entire collection of families with those from WGS of 105 families. After filtering, we defined a high-confidence set

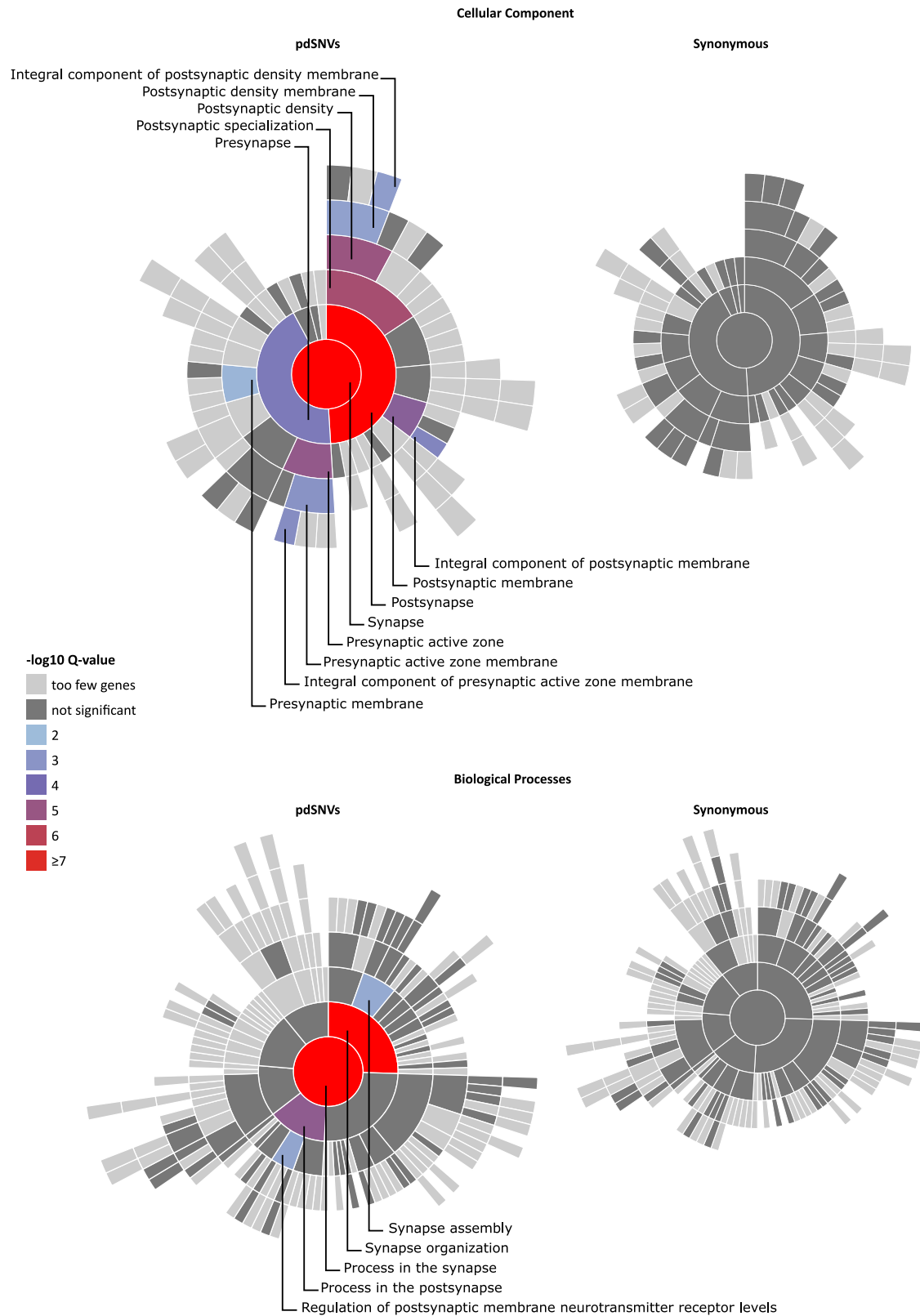
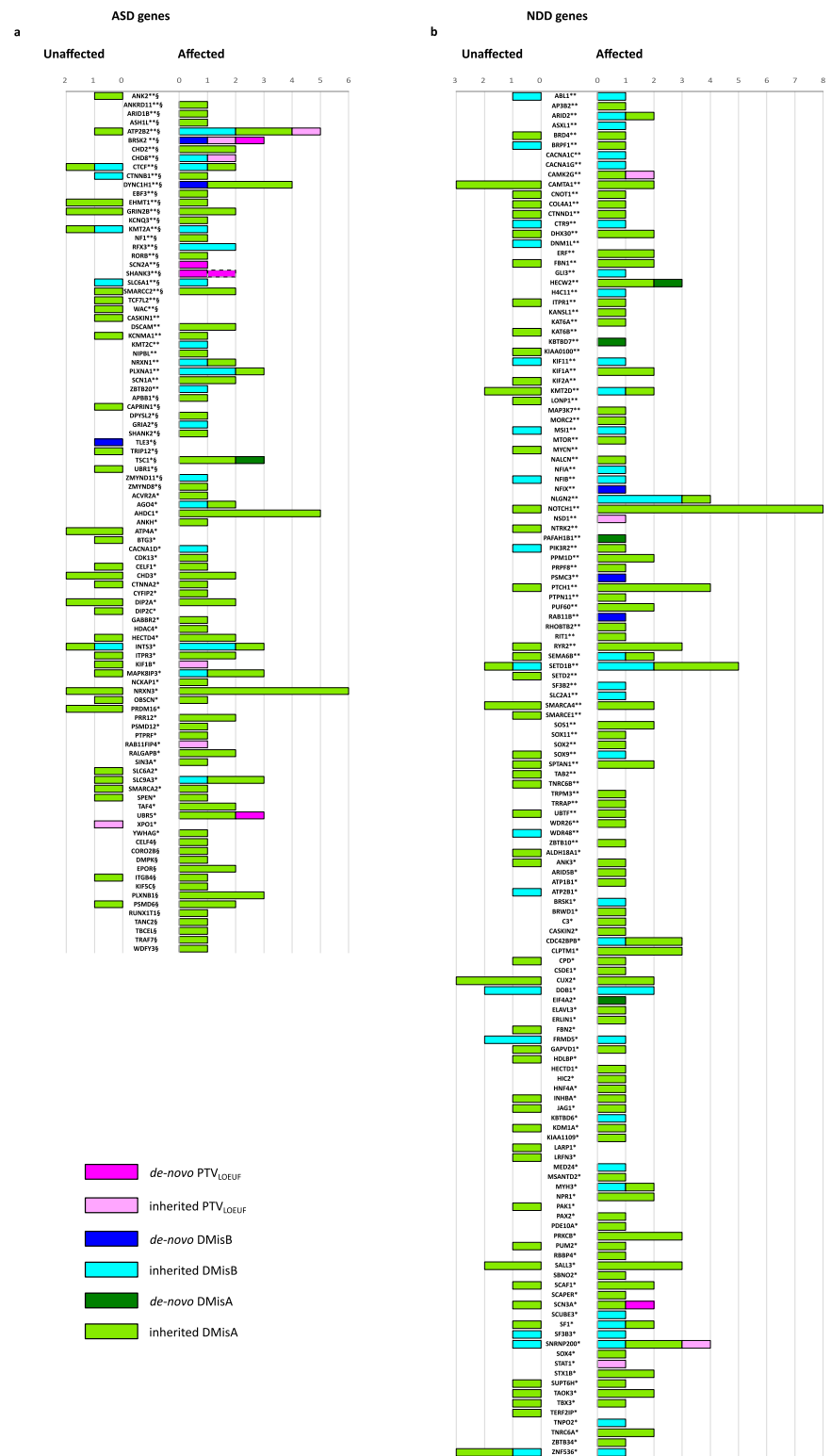


Fig. 2 | Enrichment for de novo and inherited pdSNVs in SynGO Genes. Visualisation of gene set enrichment analyses (GSEA) of genes harbouring pdSNVs (left) and synonymous variants (right) in affected individuals, each compared to a background set of brain-expressed genes. All Cell Components (CC) or Biological Process (BP) related terms with gene annotations in SynGO are plotted in a circular fashion, with the highest hierarchical term (“synapse” for CC or “process in synapse”

for BP) in the centre and each layer of subclasses in outward concentric rings. Over-represented synaptic terms are indicated with different colours, according to the Q-value, and are reported in detail in Supplementary Table 7. The CC and BP plots of genes affected by rare pdSNVs (left) show an enrichment of synaptic terms, while no enrichment emerged from the genes hosting rare synonymous SNVs (right).

Fig. 3 | Contribution of de novo and inherited pdSNVs to high confidence ASD/NDD genes. De novo and inherited pdSNVs include PTVs in genes with LOEUF score <0.6 (PTV_{LOEUF}), missense variants with MPC ≥ 2 (DmisB) and missense variants with 1 ≤ MPC < 2 (DmisA). Contribution of each variant type identified in ASD individuals and unaffected siblings for a list of genes previously associated to ASD (a) and NDD (b). The list of ASD genes comprised 185 genes associated at FDR ≤ 0.05⁵ and 135 genes with FDR < 0.1⁶ (88 of which were common between the two lists). In our cohort, pdSNVs were identified in 97 ASD genes (a). The list of NDD genes included 452 genes from a list of 664 genes associated at FDR ≤ 0.05, after the exclusion of the genes already included among the 232 ASD genes⁵. In our cohort, pdSNVs were identified in 139 NDD genes (b). **, genes with FDR ≤ 0.001⁵; *, genes with FDR ≤ 0.05⁵; §, genes with FDR < 0.1⁶; dotted line indicates a putative de novo PTV_{LOEUF}.



of 192 rare (frequency < 1% in our dataset) genic CNVs in cases and SLD siblings (Supplementary Table 10). These included 93 CNVs identified by both SNP-array and WGS, 79 detected only by WGS and 20 identified only by SNP-array in families not analysed by WGS. Among variants detected only by WGS, 32 (40.5%) were deletions (median size=20.2 kb) and 47 (59.5%) duplications (median size=31.7 kb).

We prioritised four categories of potentially damaging CNVs (pdCNVs) (Table 2):

a) **Large CNVs** (≥ 3 Mb). Proband with large CNVs were not present in our cohort, because most of them had been previously screened by array-CGH in a clinical setting. However, we identified a 3.2 Mb de novo tandem duplication of chr18p11 in one SLD sibling diagnosed with language and learning delay (Supplementary Fig. 9).

Table 2 | Potentially damaging CNVs (pdCNVs) identified in our cohort

CytoBand	Coordinates (hg38)	Detection	Individual (Family)	RefSeq Genes ^{a,b}	ACMG ^c
a) Large CNVs					
18p11.22-p11.21	NC_000018.10:g.(9291609_12509914)_(12509915_15728221)dup	SNP/WGS ^o	9.4 (f/m/aM/dM/uF)	31 genes[GNAL ; PPP4R1 ; RALBP1]	LP
b) Recurrent Genomic Loci (RGD)					
2p16.3	NC_000002.12:g.(49962600_50756048)del	SNP ^f	2.3 (f/m/aF)	2 genes[NRXN1 ; MIR8485]	LP
15q11.2	NC_000015.10:g.(22636123_23102073)_(23102074_23568025)dup	SNP/WGS	99.4 (f/m/aM/aM)	6 genes[CYFIP1]	VUS
15q11.2	NC_000015.10:g.(22636123_23117882)del	SNP ^f	117.3 (f/m/aM/aF)	6 genes[CYFIP1]	LP
15q13.2-q13.3	NC_000015.10:g.(30626840_32222140)del	SNP ^f	115.3 (f/m/aF/aM/aF)	12 genes	LP
15q13.2-q13.3	NC_000015.10:g.(30635159_32222140)_(32222141_33809123)dup	SNP/WGS	81.3 (f/m/aM/uM)	12 genes[OTUD7A]	VUS
16p11.2	NC_000016.10:g.(29584162_30188392)del	SNP ^f	118.4 (f/m/aM/aF/uM)	32 genes[TAOK2 ; MAZ]	P
c) de novo CNVs^d					
5q21.3	NC_000005.10:g.(108496181_109233820)_(109233821_109971461)dup	SNP/WGS ^o	73.3 (f/m/aF/dM)	<i>FER</i> , <i>LINC01023</i>	VUS
2p16.2	NC_000002.12:g.(54193480_54356405)del	SNP ^{f,h}	120.4 (f/m/aM/aM)	<i>ACYP2</i> , <i>C2orf73</i> , <i>TSPYL6</i>	VUS
d) CNVs including dosage-sensitive NDD genes					
1p36.13	NC_000001.11:g.(18606250_19018007)del	SNP ^f	91.3 (m/aM/dM/aM/dM)	6 genes[ALDH4A1 ; PAX7]	VUS
1p31.1	NC_000001.11:g.(71519763_71888101)del	SNP/WGS ^h	108.3 (f/m/aM)	NEGR1 , <i>NEGR1-IT1</i>	VUS
1q42.13	NC_000001.11:g.(230095012_230188321)_(230188322_230281632)dup	SNP ^f	2.3 (f/m/aF)	GALNT2	VUS
1q44	NC_000001.11:g.(245334797_245424055)del	SNP/WGS	71.3 (f/m/aF)	KIF26B	VUS
2p25.3	NC_000002.12:g.(196082_261610)del	SNP/WGS	100.3 (f/m/aF)	SH3YL1	VUS
2p25.3	NC_000002.12:g.(1736572_1846326)_(1846327_1956082)dup	WGS ^o	84.3 (f/m/aF)	<i>MYT1L</i> , <i>PXDNI</i>	VUS
2p25.2	NC_000002.12:g.(6833046_6845996)del	WGS ^o	113.4 (f/m/aF/raM/uF)	CMPK2 , <i>NRIF</i>	VUS
4q31.3	NC_000004.12:g.(150267053_150327676)_(150327677_150388301)dup	SNP/WGS	11.3 (f/m/aM/uM)	LRBA ⁱ	VUS
5q14.1	NC_000005.10:g.(79401623_79420576)del	WGS ^{o,g}	82.3 (f/m/aM/uF)	HOMER1	VUS
6q12	NC_000006.12:g.(63563200_63698372)del	SNP ^{f,h}	117.3 (f/m/aM/aF)	PHF3 , PTP4A1 , <i>LOC128125822</i>	VUS
6q25.3	NC_000006.12:g.(156870642_156885949)del	SNP/WGS	56.3 (f/m/aF/aM)	ARID1B	VUS
7q32.1	NC_000007.14:g.(127719389_127968829)del	SNP/WGS	109.3 (f/m/aM)	SND1	VUS
8q22.3	NC_000008.11:g.(104392687_104406426)del	SNP/WGS	85.3 (f/m/aM/aM)	DPYS	VUS
9p24.2	NC_000009.12:g.(2726669_2792829)del	SNP/WGS	14.3 (f/m/aM/aM)	KCNV2	VUS
9p21.1-p13.3	NC_000009.12:g.(33140780_33262543)_(33262544_33384308)dup	SNP/WGS	46.3 (f/m/aM/uM)	<i>BAG1</i> , <i>B4GALT1</i> , <i>B4GALT1-AS1</i> , <i>SPINK4</i> ⁱ	VUS
9q22.32	NC_000009.12:g.(95221201_95255683)del	SNP/WGS	96.3 (f/m/aM/uF)	FANCC	VUS
10p15.2	NC_000010.11:g.(3040783_3121006)del	SNP/WGS	17.3 (f/m/aM/uM)	PFKP , <i>PFKP-DT</i>	VUS
10q24.1	NC_000010.11:g.(95440563_95689410)_(95689411_95938259)dup	SNP/WGS	47.3 (f/m/aM)	ALDH18A1 , <i>SORBS1</i> , <i>TCTN3</i> ^j	VUS
10q24.32	NC_000010.11:g.(102640823_102666335)_(102666336_102691849)dup	WGS ^o	67.3 (f/m/aM/uF)	TRIM8	VUS
10q25.2-q25.3	NC_000010.11:g.(113078246_113111305)del	WGS ^o	47.3 (f/m/aM)	TCF7L2	VUS
13q31.3	NC_000013.11:g.(93533137_93587893)_(93587894_93642651)dup	SNP/WGS	94.3 (f/m/aM)	GPC6	VUS
16p13.2	NC_000016.10:g.(8446703_8794331)del	SNP/WGS	105.3 (f/m/aM)	ABAT , <i>TMEM114</i> , <i>METTL22</i>	VUS
16q23.1	NC_000016.10:g.(78256339_78314555)del	SNP/WGS	45.3 (f/m/aM/uF)	WWOX	VUS
20q13.33	NC_000020.11:g.(62821525_62833156)del	SNP/WGS	96.3 (f/m/aM/uF)	COL9A3	VUS
21q22.11	NC_000021.9:g.(31165520_31653872)del	SNP/WGS	55.3 (f/m/aM/aM/dM)	TIAM1 , <i>TIAM1-AS1</i>	VUS
21q22.3	NC_000021.9:g.(46140262_46168679)del	SNP/WGS	64.3 (f/m/aM)	FTCD , <i>FTCD-AS1</i> , <i>SPATC1L</i>	VUS

The CNVs reported in this table are divided according to the 4 categories used for the prioritization: variants larger than 3 Mb, variants in known recurrent genomic loci (RGD), de novo variants, variants overlapping dosage-sensitive GeneTrek genes (<https://genetrek.pasteur.fr/>). GeneTrek classification for genes included in CNVs is reported in Table S10. Dosage-sensitive genes are defined according to pHaplo and pTripto gene scores (pHaplo ≥ 0.55 for genes in CNVs potentially disrupting the CDS, pTripto ≥ 0.68 for duplications including the entire CDS of genes). Proband is indicated with an identifier code formed by the family number and the individual number. In the segregation column, children are listed sequentially after the father and the mother, according to recruitment order. Family members carrying the CNV are underlined; if the CNV is a de novo variant, the heterozygote is also indicated in bold. *a* affected, *u* unaffected, *d* specific learning disability, *M* male, *F* female, *f* father, *m* mother, *r* relative (uncle), *SNP* SNP data analysis, *WGS* genome sequencing data analysis.

Symbols: ^aGeneTrek dosage-sensitive genes according to pHaplo or pTripto scores are indicated in bold; ^bif more than 5 genes are affected by the CNV, only dosage-sensitive GeneTrek genes are listed (in brackets); ^cClassification of genetic variants according to the ACMG guidelines; *P* pathogenic, *LP* likely pathogenic, *VUS* variant of uncertain significance; ^dDe novo CNVs not included in previous categories (a and b); ^eCNV validated by Sanger sequencing; ^fCNV detected only from SNP data because WGS was not carried out for the family; ^gCNV detected only from WGS data; ^hCNV validated by qPCR; ⁱPossible intragenic duplication of haplo-insufficient GeneTrek genes; ^jPossible gene fusion including GeneTrek dosage-sensitive genes.

b) **Recurrent CNVs.** This category included 4 deletions and 2 duplications consistent with known RGD.

c) **De novo CNVs.** In addition to the two de novo CNVs included in the previous categories, we identified a 5q21.3 tandem duplication including the entire *FER* gene and a 2p16.2 deletion affecting the brain-expressed gene *ACYP2*.

d) **Rare CNVs affecting dosage-sensitive NDD genes reported in GeneTrek²¹.** This category included 19 deletions and 7 duplications, selected among deletions or intragenic duplications potentially disrupting the CDS of genes with $p\text{Haplo} \geq 0.55^{22}$, duplications involving the whole CDS of genes with $p\text{Tripl} \geq 0.68^{22}$ and CNVs potentially leading to in frame fusion transcripts. Among these, the inherited deletions involving *PHF3*, *NEGR1*, *HOMER1* and *TIAM1* are of particular interest, as these neurodevelopmental genes have been previously implicated in ASD/NDD.

Multiple hits in families with CNVs in genomic disorders loci

Since CNVs in RGD loci are often inherited and require secondary hits to reach the liability threshold for disease, we checked whether the probands heterozygote for these CNVs also had de novo pdSNVs, PTV_{LOEUF} in NDD genes or pdCNVs inherited from the parent not transmitting the recurrent CNV. Four families carried additional variants of interest (Supplementary Fig. 10). In Fam81, the proband had a likely causative de novo DmisB variant in *NFIX*, which allowed us to redefine his phenotype as Malan syndrome²³, while supporting the ACMG classification of 15q13.3 duplications as VUS. In Fam117, both affected children inherited a paternal 15q11.2 deletion and a maternal exonic deletion of *PHF3*. Moreover, each of them had a de novo Dmis, one in *YMEIL1* and the other in *RCCD1* (Table 1, Supplementary Fig. 10). Interestingly, their father exhibited autistic traits: according to the SCDC test^{13,24}, he had social and communication difficulties (SCDC score =15, an outlier in the SCDC parents' score distribution) (Supplementary Fig. 3b), while in the BAPQ¹⁴ he exhibited impairments in the pragmatic language domain.

Autosomal and X-linked recessive events

To identify variants potentially acting with a recessive inheritance, we looked for homozygous and compound heterozygous pdSNVs/pdCNVs.

Biallelic pdSNVs events were identified in six genes (Supplementary Table 11): five harboured biallelic inherited DmisA, while *DYNCH1* harboured a maternal DmisA and a de novo DmisB. However, *DYNCH1* has been reported to act through a dominant mode of inheritance, therefore the de novo DmisB is likely to be the main causative variant for the ASD phenotype in this individual²⁵.

A compound pdCNV-pdSNV event was identified in Fam91, where proband 91.3 carries a 412 kb deletion of unknown origin (paternal DNA was unavailable) and a maternal DmisA in the remaining allele of *PAX7*, a gene labelled as having a biallelic mode of inheritance in Genomics England neurology and NDD panel.

Considering only variants with no homozygotes reported in gnomAD and the mode of inheritance previously associated with these genes, only biallelic events in *PAX7* and *DSCAM* met the selection criteria (Supplementary Table 11).

To identify potentially causative X-linked events, we searched for hemizygous pdSNVs and pdCNVs present in male probands and absent in unaffected brother(s) (Supplementary Table 12). We identified 4 DmisB and 28 DmisA: 16 of these are absent in males in gnomAD (v2.1.1/v3.1.2), 12 of which map in GeneTrek NDD genes.

Polygenic risk scores

To analyse the contribution of common genetic variants to ASD risk, we calculated PRS from the individuals of European ancestry of our sample using summary statistics from a recent ASD GWAS². To test technical reproducibility, we compared PRS in two MZ twin pairs, and no between-twin difference was detected. Even if the small difference in mean PRS between cases and unaffected sibs was not significant (Supplementary Fig. 11a), we observed a significant PRS over-transmission in cases ($n = 103$,

pTDT mean=0.20, p value = 0.04), but not in unaffected siblings ($n = 44$, mean=0.11, p value = 0.39) (Supplementary Fig. 11b). Considering SPX and MPX separately, we did not observe a significant PRS over-transmission in any of the two groups, likely due to the limited sample size, especially for the MPX group (SPX: 78 probands, pTDT mean=0.14, p value = 0.21; MPX: 25 probands, pTDT mean=0.43, p value = 0.06).

Discussion

We report an integrated analysis of rare protein-coding SNVs, indels and CNVs from WGS/WES and SNP-array data of a cohort of 116 ASD families. This analysis led to the identification of potentially damaging de novo and inherited variants expanding the allelic diversity and the mode of inheritance of specific ASD/NDD risk genes, while helping characterise their phenotypic impact. Moreover, the identification of de novo pdSNVs of high functional severity in 8 genes (*AGPAT3*, *IRX5*, *MGAT5B*, *RAB8B*, *RAP1A*, *RASAL2*, *SLC9A1*, *YMEIL1*) not previously described as high-confidence ASD/NDD genes^{5,6,22} highlighted promising candidates (Table 1). Among these, *RAB8B*, *RAP1A* and *SLC9A1* were also listed among the genes driving significantly enriched biological processes “regulation of transport” and “regulation of localization” in our GO enrichment analysis (Supplementary Table 5).

To better interpret the role of the de novo pdSNVs identified in this study, and in particular those in candidate genes, we annotated the genes harbouring these variants with the associated diseases from OMIM, and any animal models with neurological phenotypes as reported in OMIM (<https://omim.org>) or IMPC (www.mousephenotype.org) (Supplementary Table 4). Among the 8 promising candidate genes, *IRX5* and *SLC9A1* have been recently implicated in neurological syndromes, although with a recessive inheritance model, and their role in brain development is confirmed by animal models (Supplementary Table 4). *IRX5* has been implicated in Hamamy Syndrome (OMIM #611174), a recessive condition including craniofacial anomalies, myopia and cognitive problems. To date, only 4 families with this syndrome have been described, all with homozygous missense variants in *IRX5*. Instead, the de novo pdSNV identified in our cohort is a high-confidence stop-gain variant located in exon 1, highly expressed in the brain. According to the LOEUF score, *IRX5* is intolerant to LoF variants, suggesting that PTVs could act with a dominant model. *SLC9A1* has been associated with Lichtenstein-Knorr syndrome (OMIM #616291), a recessive neurological disorder characterized by progressive cerebellar ataxia. Three families have been reported with this syndrome, two with homozygous LoF^{26,27} and one with a homozygous missense variant shared by three siblings²⁸. However, de novo missense variants in *SLC9A1* have been identified in two individuals with seizures and other developmental disorders, including ASD^{29,30}, suggesting a possible association between de novo heterozygous variation in *SLC9A1* and NDDs. In addition, *RAP1A* has been implicated in Kabuki syndrome (KS) by a zebrafish Rap1a knockout model and the identification of a case with a homozygous missense variant due to uniparental disomy³¹. Given the residual basal activity, the variant was hypothesized to be a hypomorphic LoF allele, while the de novo PTV identified in our study is predicted to cause a complete LoF, and therefore might be the major determinant of the ASD phenotype, even if in a heterozygous status.

Among the 37 de novo pdSNVs detected in affected individuals, 15 were in high-confidence ASD/NDD genes^{5,6}. Interestingly, two of them (one PTV and a DmisB) occurred in the same gene, *BRSK2*. The identification of two de novo events in *BRSK2* in two different families is noteworthy given that *BRSK2* is highly constrained with only 29 de novo missense and PTV variants reported to date^{5,6,8,32-36} (Fig. 4). The frameshift variant is novel, while the DmisB variant has been reported in gnomAD v3.1.2 in one individual recruited as a case in a neurologic/psychiatric study (gnomAD “neuro” dataset). Intriguingly, large sequencing studies comparing the genetic architecture of ASD with other NDDs to discriminate between genes predominantly underlying ASD and those affecting development more broadly have found evidence for *BRSK2* only from ASD cohorts⁵. Therefore, a possible explanation for the high frequency of *BRSK2* rare de novo

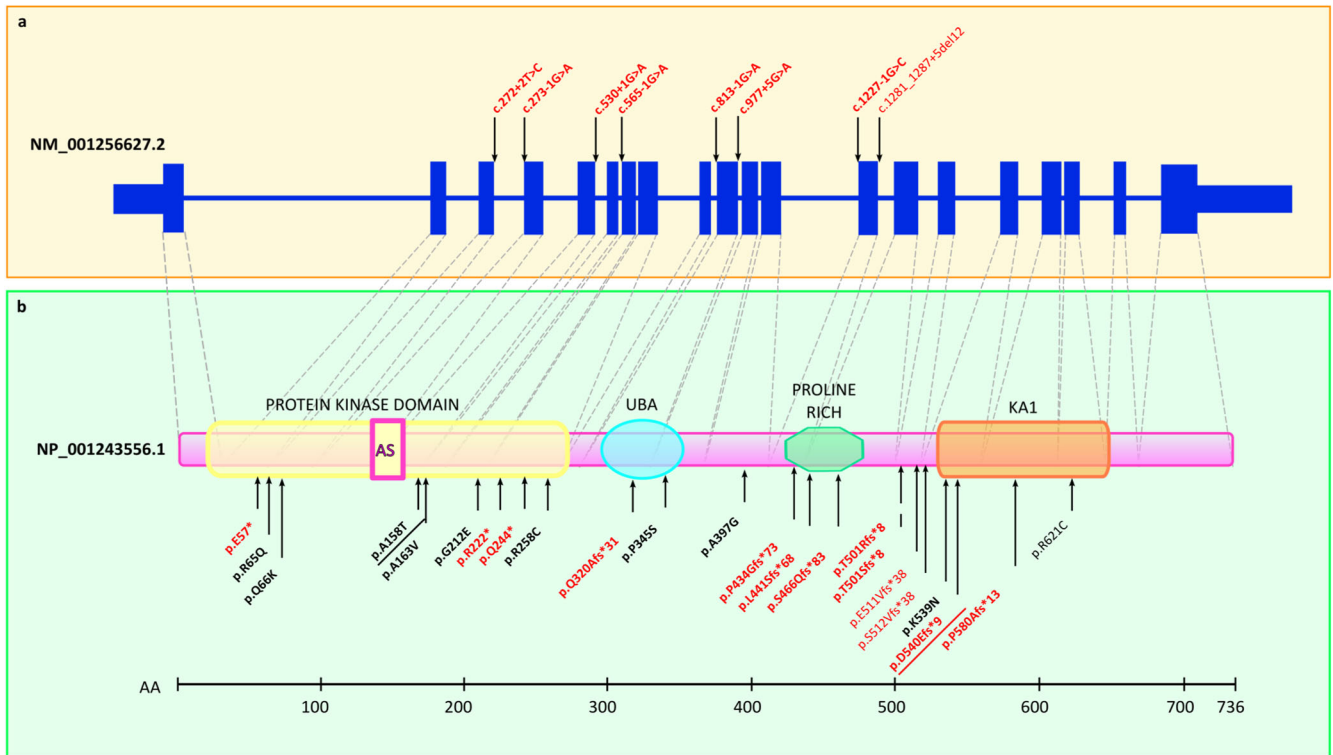


Fig. 4 | BRSK2 exons, domains and reported variants. Schematic representation of the *BRSK2* gene structure (a) and protein domains (b), illustrating potentially damaging variants reported in this and previous studies. Protein domains include protein kinase domain (containing the active site, AS), ubiquitin-associated domain (UBA), proline-rich domain (Pro-Rich), and kinase-associated 1 (KA1) domain.

Splice variants are shown above the schematic representation of the MANE transcript (upper panel), and protein-altering variants are shown below the schematic representation of *BRSK2* (PTVs in red, missense variants in black). Confirmed de novo variants are highlighted in bold. The two variants identified in this study (p.(Ala158Thr), p.(Asp540GlufsTer9)) are underlined.

mutations in our study is that our cohort was specifically ascertained for ASD. Moreover, the two probands with *BRSK2* de novo pdSNVs have both idiopathic ASD and no comorbidities (Supplementary Information). Taken together, these data support the hypothesis that *BRSK2* belongs to a set of genes that, when disrupted, alter the core features of ASD and thus are particularly promising for neurobiological studies of ASD. *BRSK2* encodes for a serine/threonine-protein kinase involved in axonogenesis and polarization of cortical neurons. Its role in neurodevelopment has been studied in mice models³⁷ and, most recently, in a *brsk2*-deficient zebrafish model that showed ASD-like behaviours³⁸.

Another de novo pdSNV of particular interest is the stop-gain variant identified in *SCN3A*, a gene predicted to be highly intolerant to LoF. This variant occurs in the last exon and while it is expected to escape nonsense-mediated decay (NMD), it is predicted to cause the loss of 371 aa involving part of the fourth transmembrane domain (177 aa) and the entire cytoplasmic C-terminal tail (Supplementary Fig. 12). Pathogenic variants in this gene lead to a spectrum of neurodevelopmental conditions including epilepsy, as well as developmental brain malformations but, to our knowledge, no PTVs in *SCN3A* have been previously reported in ASD individuals. The clinical description of proband 40.3 is reported in Supplementary Information.

In addition to expanding the spectrum of potentially damaging variants in recently implicated ASD/NDD genes, this study also helps clarify their mode of inheritance. An example is given by the heterozygous deletion disrupting *PHF3* identified in Fam117 (Table 2). This gene encodes a PHD finger protein that regulates transcription and mRNA stability and is involved in the timely expression of neuronal genes during neurogenesis³⁹. *PHF3* is a high-confidence ASD gene (Supplementary Table 8); its strong association with ASD (FDR < 0.1) was mainly driven by de novo PTVs⁵. Rare inherited PTVs in *PHF3* are also associated to ASD risk, as shown by Transmission Disequilibrium Test (TDT) in 13,000 ASD families⁸. Taken

together, these data suggest that *PHF3* belongs to a subset of ASD genes increasing risk through both de novo and inherited PTVs. The maternal *PHF3* deletion identified in our cohort provides further support to the role of inherited deleterious variants in this gene. Notably, the inheritance pattern observed in our family suggests an incomplete penetrance, likely to be modulated by other risk factors. Indeed, in Fam117 we identified additional rare inherited and de novo risk variants that might contribute to the cognitive and behavioural phenotypes of the two affected children with the deletion (Supplementary Fig. 10).

Our CNV analysis also provides additional support to inherited variants in the candidate-NDD gene *NEGR1*. We identified a maternally inherited intragenic deletion in the simplex family 108 (Table 2). Previous studies have reported similar *NEGR1* microdeletions, inherited or of unknown origin, in individuals with developmental delay, ID and autistic features^{40,41}. *NEGR1* was also highlighted by the largest GWAS meta-analysis performed to date for ASD as the only protein-coding gene of the four genome-wide significant loci shared between ASD and major depression². *NEGR1* is a cell adhesion protein involved in neurite outgrowth regulation, dendritic arborization and synapse formation⁴². Interestingly, *Negr1* deficiency in mouse results in abnormal neuronal growth and migration, abnormal spine density during cortical development and impaired social behaviour^{43,44}.

The identification of an inherited deletion disrupting *TIAMI* is also of interest (Table 2). This gene encodes a guanine nucleotide exchange factor (GEF) that regulates RAC1 signaling pathway, which affects neuronal morphogenesis and neurite outgrowth¹⁵. *TIAMI* has been recently implicated in NDDs by a study reporting biallelic missense variants in 5 individuals with ID, language delay and seizures. Functional studies of three of these variants showed only a partial LoF effect⁴⁵. In contrast, our deletion is predicted to determine a total LoF and thus might have a severe impact, even if monoallelic. The intolerance of *TIAMI* to LoF events is supported by high

pHaplo score and by the absence of exonic deletions in gnomAD and DGV. Taken together, these data suggest that *TIAM1* LoF events may contribute to NDD risk but with a reduced penetrance.

Given the complex architecture of ASD, where a diverse spectrum of variants contributes to the susceptibility, even within the same individual, WGS represents the ideal approach for a comprehensive investigation of all sizes and types of variants underlying the risk.

Notably, 18.5% of pdCNVs (5/27 CNVs identified in 105 families characterized with both WGS and SNP-array) would not have been detected without WGS, highlighting the benefits of WGS for the detection of smaller CNVs. Among these, WGS identified an exonic deletion of 19 kb in *HOMER1* not found from SNP data as only two probes map inside the deletion (Table 2, Supplementary Fig. 13). *HOMER1* is a key component of the postsynaptic density (PSD), where it exerts an important scaffolding role, interacting with multiple targets, including SHANK proteins⁴⁶. The proband, who has a moderate early-onset autism (ADOS-2 comparison Score=6) without cognitive impairment (LEITER-R=102), shares the deletion with the unaffected sister, who do not present autistic features or cognitive impairment, suggesting that it may act as a susceptibility factor with incomplete penetrance.

The clinical relevance of de novo pdSNVs/pdCNVs and recurrent CNVs was interpreted according to the ACMG guidelines⁴⁷. Six pdSNVs and 1 CNV were classified as pathogenic while 30 pdSNVs and 3 CNVs as likely pathogenic (Table 1 and Table 2). Of these, 19 variants were in high-confidence ASD-NDD genes or RGD loci, providing a molecular diagnosis in 19/144 ASD cases. This diagnostic yield (13%) is consistent with previous estimates³, although most likely represents an underestimate of the true etiologic yield, since all probands were pre-screened by clinical aCGH and excluded if positive. Moreover, continuous discovery efforts and functional studies may help to clarify the role of the other 21 pathogenic/likely pathogenic variants, establishing their diagnostic relevance, increasing the current yield, and implicating new ASD risk genes. Notably, among the pathogenic variants, the de novo DmisB identified in exon 2 of *NFIX* prompted us to reassess the phenotype of the proband in Fam81, leading to a clinical diagnosis of Malan syndrome. This proband has early-onset severe autism, profound ID, dysmorphic features, macrocephaly and mild brain MRI anomalies, consistent with the main features of Malan syndrome^{23,48} (Supplementary Information).

Given the small size of our cohort, we have limited power in performing aggregate analysis of rare variants. Nevertheless, SynGO analysis of the rare de novo and inherited pdSNVs identified in affected individuals showed a significant enrichment in genes involved in synaptic components and processes, in contrast with the genes harbouring rare synonymous variants that did not display any synaptic enriched terms. Since synaptic dysregulation is widely recognized as an important component of ASD risk, this finding supports the pathological role of the pdSNVs identified in synaptic genes.

We also evaluated the frequency of pdSNVs in a list of high-confidence ASD/NDD genes, identifying a higher rate of rare de novo pdSNVs in the 144 cases compared to the 55 unaffected siblings (11% versus 1.8%). Moreover, probands carrying de novo pdSNVs and those with severe pdSNVs (regardless of inheritance status) were more likely to have severe ID. This finding aligns well with the observation that de novo variants are more frequently found in ASD cases with comorbidities and support a role for inherited more deleterious pdSNVs in cases with more severe phenotypes⁴⁹.

WGS data were also used to compute PRS. The significant over-transmission of common risk variants from parents to ASD children is consistent with previous results⁵⁰ and supports the additive role of common genetic variants in ASD susceptibility.

Our results should be interpreted in the context of the small sample size (116 families), which is the principal limitation of this study. Our cohort obviously is not sufficient to achieve statistical significance for the implication of new risk genes. However, our family-based study provides valuable new data on the allelic diversity and mutational mechanisms that impact

specific genes contributing to ASD and NDDs, strengthening their involvement in these disorders and offering interesting insights into the genomic architecture underpinning ASD. Moreover, we identified potentially damaging variants in promising candidate genes that warrant further investigation.

Methods

Clinical assessment and description of samples

The cohort analysed in this study consisted of 116 ASD families recruited by “UOSI Disturbi dello Spettro Autistico” (IRCCS Istituto delle Scienze Neurologiche, Bologna, Italy).

This study was approved by the local Ethical Committee (Comitato Etico di Area Vasta Emilia Centro (CE-AVEC); code CE14060) and performed in compliance with all relevant ethical regulations including the Declaration of Helsinki. All participants or substitute decision makers provided a written informed consent to participate to the study. Written consent was obtained for publication of the photographs of probands with *BRSK2*, *SCN3A* and *NFIX* de novo variants (Supplementary Fig. 14). For each family, we collected blood samples from all available family members, for a total of 435 individuals.

Clinical diagnoses were given by a team of clinicians according to the Diagnostic and Statistical Manual of Mental Disorders 5th edition (DSM-5)⁵¹. Specifically, ASD subjects were assessed using a set of standardized clinical tests to evaluate the presence and severity of ASD (Autism Diagnostic Observation Schedule-Second Edition, ADOS-2⁵² and The Childhood Autism Rating Scale-Second Edition, CARS-2⁵³), to assess both developmental/cognitive levels (Bayley, PEP-3, Leiter-R, Griffith Scales, Wechsler Scales) and adaptive behaviour (Vineland Adaptive Behavior Scale, VABS)⁵⁴ as well as discrete and clinical signs like mimicry, hyperactivity, sensory abnormalities and symptoms age onset⁵⁵. Since measures of IQ were quantified using multiple methods, we also converted full-scale scores from different scales into five IQ categories (severe, moderate, mild, borderline and normal).

Family members were assessed for subclinical features using the Social and Communication Disorders Checklist (SCDC)¹³ and The Broad Autism Phenotype Questionnaire (BAPQ)^{14,56}.

Electroencephalogram (EEG) and Magnetic Resonance Imaging (MRI) were also performed on 126 and 125 ASD individuals, respectively.

Genotyping data processing

All genetic analyses were performed on DNA samples extracted from whole blood using a QIAamp DNA blood kit (Qiagen, Hilden, Germany).

The whole cohort ($n = 435$ individuals) was genotyped using the Illumina Infinium PsychArray-24 v1.3 BeadChip. Genotyping quality control was performed according to standard procedures⁵⁷. Briefly, we excluded markers that exhibited high missingness rates (>5%), low minor allele frequency (<1%), or failed a test of Hardy-Weinberg equilibrium ($p < 1 \times 10^{-5}$). No individuals were excluded due to a high proportion of missing genotype data ($\geq 2\%$), inconsistent sex information or for high rates of heterozygosity (>3sd from the mean).

Ancestry determination

SNP data were used to determine the ancestry of all individuals of our cohort with PLINK⁵⁸. We first removed large-scale high-Linkage Disequilibrium (LD) regions and performed LD pruning using the option ‘--indep-pairwise 50 5 0.2’. Then, we performed genome-wide pairwise IBS calculations and multidimensional scaling (MDS) analysis, anchoring our cohort data to the data of the 1000 Genomes Project (20100804 release) (<http://www.1000genomes.org/>) to visualize genetic distances.

Sequencing, quality control, variant calling and annotation

WGS was performed on 105 families, while WES was carried out for 29 families, with 18 families being analysed with both.

WES was performed using the NimbleGen SeqCap EZ MedExome enrichment kit (Roche) and Illumina NextSeq500 or HiSeq sequencers. All

exomes had a read depth (DP) > 10x for 90% of the total exome coverage and > 20x for 80%. Data analysis was performed using CoVaCS⁵⁹, a pipeline exploiting three different calling algorithms (GATK, Varscan and FreeBayes) to generate a final set of high-confidence variants.

WGS was performed at the New York Genome Center. Alignment and post-processing were carried out using the standard pipeline for the CCDG⁶⁰ and the GRCh38_full_analysis_set_plus_decoy_hla.fa reference genome. Briefly, raw reads were aligned to the GRCh38 reference genome (Burrows–Wheeler Aligner–MEM)⁶¹, duplicate reads were marked (Picard v.2.4.1, <http://broadinstitute.github.io/picard/>), base scores were recalibrated and indels were realigned (GATK v.3.5.0)⁶². SNVs and indels were called using the GATK HaplotypeCaller and FreeBayes v1.1.0 (<https://github.com/ekg/freebayes>) on a per-family basis. After some basic sample-level filtering (DP > 9 for parents and children, child genotype quality (GQ) > 20, child allele balance (AB) > 0.25, parent alternate allele count (AO) = 0), de novo variants were retained only if they had been identified by both GATK and FreeBayes.

Variant annotation was performed with ANNOVAR⁶³, using RefSeq for gene-based annotation (Genome Build hg38). Annotated variants were filtered in order to retain only coding and splicing variants, and to remove low-quality variants (Coverage (DP) < 10, Genome Quality (GQ) < 20 and Variant Quality Score Recalibration (VQSR) not indicating PASS). We also removed variants located in regions known to be difficult for variant calling (HLA, mucins, and olfactory receptors).

Rare variants were defined according to the population allele frequencies in the non-neurological subset of gnomAD v.2.1.1 and the entire dataset of gnomAD v.3.0; MAF thresholds of $\leq 0.1\%$ and $\leq 1\%$ were applied to analyse variants according to a monoallelic (dominant or X-linked hemizygous) or biallelic model, respectively.

To evaluate the impact of rare coding variants on gene function, we used the LOEUF (loss-of-function observed / expected upper bound fraction) score¹⁶ to rank the protein truncating variants (PTVs, including stopgain, stoploss, frameshift and canonical splice site variants) in 2 bins of severity (using a threshold of LOEUF < 0.6) and the integrated “missense badness, PolyPhen-2, constraint” (MPC) score¹⁷, to rank the missense variants in other 3 bins of severity (MPC ≥ 2 (DmisB), $1 \leq \text{MPC} < 2$ (DmisA), $0 \leq \text{MPC} < 1$). To further assess the potential relevance of de novo most deleterious variants (PTV_{LOEUF}, DmisB, DmisA), we used the LOFTEE¹⁶ annotation to identify high-confidence LoF variants, the pext (mean proportion expressed across transcripts) score¹⁸ to assess if a variant occurs in a brain expressed exon and AlphaMissense¹⁹ annotations to predict missense variant pathogenicity by combining structural context and evolutionary conservation (Supplementary Table 4).

Genes previously associated with ASD or other NDDs were retrieved from gene lists compiled from two recent large WES and WGS studies on ASD/NDD^{5,6} and from “GeneTrek” (<https://genetrek.pasteur.fr/>), a website centralizing NDD gene lists from the most relevant databases. All the de novo variants DNVs of interest were visually inspected using IGV⁶⁴. De novo PTVs in constrained genes (PTV_{LOEUF}) and other selected de novo missense variants were also validated by Sanger sequencing.

Polygenic risk score

We calculated Polygenic Risk Scores (PRS) in 356 individuals of European ancestry, with WGS data available. We used the additive model implemented in PLINK v.1.9⁵⁸ and the summary statistics from a large genome-wide association study (GWAS)² performed in ASD individuals of European ancestry. Prior to these analyses, we performed standard quality control steps⁶⁵. Briefly, we excluded variants with MAF ≤ 0.01 or imputation INFO score ≤ 0.8 and ambiguous SNPs to avoid potential strand conflicts. Clumping was performed using an r^2 threshold of 0.1 and a radius of 250 kb. Only SNPs with a p -value ≤ 0.01 were used for PRS computation. Each genotype was weighted with the variant’s OR and all the weighted variants were summed together into a PRS. The polygenic Transmission Disequilibrium Test (pTDT) was performed as previously described⁵⁰. We evaluated pTDT test statistic as a two-sided, one-sample t test.

CNV data analysis

For CNV identification we used two types of data: the Illumina Infinium PsychArray SNP data (available for the whole cohort, $n = 435$ individuals) and WGS data (available for 105 families, $n = 392$ individuals).

For SNP-array data, CNVs were identified as previously described⁶⁶. Briefly, we used three different calling algorithms: PennCNV⁶⁷, QuantiSNP⁶⁸ and CNVPartition (Illumina). We then generated a stringent set of CNVs, defined as those called by ≥ 2 algorithms (with one being PennCNV) with moderately high confidence (confidence scores ≥ 10 , CNV size $\geq 1\text{Kb}$ and number of consecutive probes for CNV detection ≥ 3) and with a reciprocal overlap at least 50%. If the CNV boundaries varied between the different calling algorithms, we retained the largest ones. CNVs were annotated for size, overlapping genes according to RefSeq, exonic content, overlap with segmental duplications, overlap with centromeric regions, overlap with known recurrent CNVs associated to neurodevelopmental disorders (defined as having at least 40% overlap with the loci reported in Supplementary Table 3 of Douard et al.⁶⁹), CNVs displayed in DGV, frequency in the stringent CNV list in our 230 ASD parents, overlap with copy-number stable regions according to the stringent CNV map of the human genome⁷⁰, and NDD gene classification according to the “GeneTrek” database. After the annotation, to reduce false-positive calls, we retained only CNVs $\geq 10\text{ kb}$ in length and including ≥ 5 consecutive probes. Moreover, we selected only CNVs including at least one RefSeq exon (exonic CNVs). The trio option of PennCNV was used to confirm inheritance status of the resulting CNV calls. All de novo rare CNVs were manually curated by visual inspection of the BAF and LRR plots and false positives were excluded.

For WGS data, CNVs $\geq 10\text{ kb}$ were detected using Canvas⁷¹, a read-depth based CNV calling tool developed by Illumina. Rare CNVs were annotated and defined with the same criteria used for microarray data. To determine the CNV inheritance status, parents and child calls were compared and all overlapping calls were identified. CNV calls in the child with no overlapping CNVs in the parents were tagged as being potentially de novo. If some overlapping calls were found in a parent, but with a reciprocal overlap < 50% or the CNV type (deletion or duplication) did not match, then the CRAM files were manually inspected to visualize the CNV region in IGV.

To resolve the structures of duplications, determine the breakpoint coordinates of selected CNVs at the base level, and understand their impact on genes, we focused on rare CNVs that overlapped exons of NDD genes reported as HC by GeneTrek. CNV calls were analysed by manual inspection of paired-end reads and split reads at the breakpoint junctions visualizing CRAM files using IGV. By using IGV color coding to flag anomalous insert sizes and pair orientations, we were able to detect deletion and duplications and to classify duplications as tandem or inverted. Duplications were considered to possibly increase gene dosage when at least one RefSeq isoform was fully contained within the duplication. The effects of partial deletions, intragenic duplications and fusion genes created at the CNV breakpoints were assessed using the CCDS track of UCSC Genome Browser.

Finally, we analysed the overlap between SNP-array and GS CNV calls. After selecting CNVs $\geq 10\text{ kb}$ in length and including at least one exon, we restricted our analyses to rare CNVs defined as either known recurrent CNVs associated to NDDs or non-recurrent CNVs with the following characteristics: (i) having an overlap with segmental duplication or centromeric regions < 50%; (ii) having a frequency $\leq 1\%$ in the 230 parents, using the 50% reciprocal overlap criteria; (iii) having more than 75% overlap with copy-number stable regions, according to the stringent CNV map of the human genome⁷⁰. CNVs identified by both methods were considered high-quality calls and were retained with the coordinates obtained by CANVAS, refined by subsequent manual inspection. CNVs deemed relevant to NDDs identified by WGS but missed by SNP-array for lack of probes in the region or identified only by SNP-array in samples without WGS data, were experimentally validated by Sanger Sequencing and SYBR® Green-based real-time quantitative PCR assays⁶⁶.

Reporting summary

Further information on research design is available in the Nature Research Reporting Summary linked to this article.

Data availability

The genomic and phenotypic data for the families analysed in this study are available by request from dbGAP (dbGaP accession [phs002509.v1.p1](https://dbgap.ncbi.nlm.nih.gov/alpha/a/gap/studies/phs002509.v1.p1)).

Received: 20 October 2023; Accepted: 27 February 2024;

Published online: 22 March 2024

References

- Lord, C. et al. Autism spectrum disorder. *Nat. Rev. Dis. Primers* **6**, 1–23 (2020).
- Grove, J. et al. Identification of common genetic risk variants for autism spectrum disorder. *Nat Genet* **51**, 431–444 (2019).
- Tammimies, K. et al. Molecular Diagnostic Yield of Chromosomal Microarray Analysis and Whole-Exome Sequencing in Children With Autism Spectrum Disorder. *Jama* **314**, 895–903 (2015).
- Satterstrom, F. K. et al. Large-Scale Exome Sequencing Study Implicates Both Developmental and Functional Changes in the Neurobiology of Autism. *Cell* **180**, 568–584.e523 (2020).
- Fu, J. M. et al. Rare coding variation provides insight into the genetic architecture and phenotypic context of autism. *Nat. Genet.* **54**, 1320–1331 (2022).
- Trost, B. et al. Genomic architecture of autism from comprehensive whole-genome sequence annotation. *Cell* **185**, 4409–4427.e4418 (2022).
- Wilfert, A. B. et al. Recent ultra-rare inherited variants implicate new autism candidate risk genes. *Nat. Genet.* **53**, 1125–1134 (2021).
- Zhou, X. et al. Integrating de novo and inherited variants in 42,607 autism cases identifies mutations in new moderate-risk genes. *Nat. Genet.* **54**, 1305–1319 (2022).
- Pinto, D. et al. Functional impact of global rare copy number variation in autism spectrum disorders. *Nature* **466**, 368–372 (2010).
- Moreno-De-Luca, D. et al. Using large clinical data sets to infer pathogenicity for rare copy number variants in autism cohorts. *Mol. Psychiatry* **18**, 1090–1095 (2013).
- Zarrei, M. et al. A large data resource of genomic copy number variation across neurodevelopmental disorders. *NPJ Genom. Med.* **4**, 26 (2019).
- Rochat, M. J. et al. Brain Magnetic Resonance Findings in 117 Children with Autism Spectrum Disorder under 5 Years Old. *Brain Sci.* **10** (2020).
- Skuse, D. H., Mandy, W. P. & Scourfield, J. Measuring autistic traits: heritability, reliability and validity of the Social and Communication Disorders Checklist. *Br. J. Psychiatry* **187**, 568–572 (2005).
- Hurley, R. S., Losh, M., Parlier, M., Reznick, J. S. & Piven, J. The broad autism phenotype questionnaire. *J. Autism. Dev. Disord.* **37**, 1679–1690 (2007).
- Caporali, L. et al. Dissecting the multifaceted contribution of the mitochondrial genome to autism spectrum disorder. *Front. Genet.* **13**, 953762 (2022).
- Karczewski, K. J. et al. The mutational constraint spectrum quantified from variation in 141,456 humans. *Nature* **581**, 434–443 (2020).
- Samochoa, K. E. et al. Regional missense constraint improves variant deleteriousness prediction. *bioRxiv*, <https://doi.org/10.1101/148353> (2017).
- Cummings, B. B. et al. Transcript expression-aware annotation improves rare variant interpretation. *Nature* **581**, 452–458 (2020).
- Cheng, J. et al. Accurate proteome-wide missense variant effect prediction with AlphaMissense. *Science* **381**, eadg7492 (2023).
- Koopmans, F. et al. SynGO: An Evidence-Based, Expert-Curated Knowledge Base for the Synapse. *Neuron* **103**, 217–234.e214 (2019).
- Leblond, C. S. et al. Operative list of genes associated with autism and neurodevelopmental disorders based on database review. *Mol Cell Neurosci.* **113**, 103623 (2021).
- Collins, R. L. et al. A cross-disorder dosage sensitivity map of the human genome. *Cell* **185**, 3041–3055.e3025 (2022).
- Priolo, M. et al. Further delineation of Malan syndrome. *Hum. Mutat.* **39**, 1226–1237 (2018).
- Riglin, L. et al. Variable Emergence of Autism Spectrum Disorder Symptoms From Childhood to Early Adulthood. *Am. J. Psychiatry* **178**, 752–760 (2021).
- Amabile, S. et al. DYNC1H1-related disorders: A description of four new unrelated patients and a comprehensive review of previously reported variants. *Am. J. Med. Genet. A* **182**, 2049–2057 (2020).
- Iwama, K. et al. A novel SLC9A1 mutation causes cerebellar ataxia. *J. Hum. Genet.* **63**, 1049–1054 (2018).
- Hesarur, N. et al. Lichtenstein-Knorr Syndrome: A Rare Case of Ataxia with Sensorineural Hearing Loss. *Ann. Indian. Acad. Neurol.* **25**, 970–973 (2022).
- Guissart, C. et al. Mutation of SLC9A1, encoding the major Na⁺/H⁺ exchanger, causes ataxia-deafness Lichtenstein-Knorr syndrome. *Hum. Mol. Genet.* **24**, 463–470 (2015).
- Zhu, X. et al. Whole-exome sequencing in undiagnosed genetic diseases: interpreting 119 trios. *Genet. Med.* **17**, 774–781 (2015).
- Li, X. & Fliegel, L. A novel human mutation in the SLC9A1 gene results in abolition of Na⁺/H⁺ exchanger activity. *PLoS One* **10**, e0119453 (2015).
- Bögershausen, N. et al. RAP1-mediated MEK/ERK pathway defects in Kabuki syndrome. *J. Clin. Invest.* **125**, 3585–3599 (2015).
- Hiatt, S. M. et al. Deleterious Variation in BRSK2 Associates with a Neurodevelopmental Disorder. *Am. J. Hum. Genet.* **104**, 701–708 (2019).
- Feliciano, P. et al. Exome sequencing of 457 autism families recruited online provides evidence for autism risk genes. *NPJ Genom. Med.* **4**, 19 (2019).
- De Rubeis, S. et al. Synaptic, transcriptional and chromatin genes disrupted in autism. *Nature* **515**, 209–215 (2014).
- Mahjani, B. et al. Prevalence and phenotypic impact of rare potentially damaging variants in autism spectrum disorder. *Mol. Autism.* **12**, 65 (2021).
- Costa, C. I. S. et al. Three generation families: Analysis of de novo variants in autism. *Eur. J. Hum. Genet.* (2023).
- Nakanishi, K. et al. Isozyme-Specific Role of SAD-A in Neuronal Migration During Development of Cerebral Cortex. *Cereb. Cortex* **29**, 3738–3751 (2019).
- Deng, J. et al. Deleterious Variation in BR Serine/Threonine Kinase 2 Classified a Subtype of Autism. *Front. Mol. Neurosci.* **15**, 904935 (2022).
- Appel, L. M. et al. PHF3 regulates neuronal gene expression through the Pol II CTD reader domain SPOC. *Nat. Commun.* **12**, 6078 (2021).
- Genovese, A., Cox, D. M. & Butler, M. G. Partial Deletion of Chromosome 1p31.1 Including only the Neuronal Growth Regulator 1 Gene in Two Siblings. *J. Pediatr. Genet.* **4**, 23–28 (2015).
- Tassano, E. et al. 1p31.1 microdeletion including only NEGR1 gene in two patients. *Eur. J. Med. Genet.* **63**, 103919 (2020).
- Kubick, N., Brösamle, D. & Mickael, M. E. Molecular Evolution and Functional Divergence of the IgLON Family. *Evol. Bioinform. Online* **14**, 1176934318775081 (2018).
- Szczurkowska, J. et al. NEGR1 and FGFR2 cooperatively regulate cortical development and core behaviours related to autism disorders in mice. *Brain* **141**, 2772–2794 (2018).
- Singh, K. et al. Neuronal Growth and Behavioral Alterations in Mice Deficient for the Psychiatric Disease-Associated. *Front. Mol. Neurosci.* **11**, 30 (2018).

45. Lu, S. et al. Loss-of-function variants in TIAM1 are associated with developmental delay, intellectual disability, and seizures. *Am. J. Hum. Genet.* **109**, 571–586 (2022).
46. Stillman, M., Lautz, J. D., Johnson, R. S., MacCoss, M. J. & Smith, S. E. P. Activity dependent dissociation of the Homer1 interactome. *Sci. Rep.* **12**, 3207 (2022).
47. Richards, S. et al. Standards and guidelines for the interpretation of sequence variants: a joint consensus recommendation of the American College of Medical Genetics and Genomics and the Association for Molecular Pathology. *Genet. Med.* **17**, 405–424 (2015).
48. Macchiaioli, M. et al. A deep phenotyping experience: up to date in management and diagnosis of Malan syndrome in a single center surveillance report. *Orphanet. J. Rare Dis* **17**, 235 (2022).
49. Robinson, E. B. et al. Autism spectrum disorder severity reflects the average contribution of de novo and familial influences. *Proc. Natl. Acad. Sci. USA* **111**, 15161–15165 (2014).
50. Weiner, D. J. et al. Polygenic transmission disequilibrium confirms that common and rare variation act additively to create risk for autism spectrum disorders. *Nat. Genet.* **49**, 978–985 (2017).
51. American Psychiatric Association, DSM-5 Task Force. Diagnostic and statistical manual of mental disorders: DSM-5™ (5th ed.). (American Psychiatric Association, Washington, D.C., 2013).
52. Lord, C. et al. (ADOS®-2) Autism Diagnostic Observation Schedule™, Second Edition (Western Psychological Services, Torrance, CA, USA, 2012).
53. Schopler, E., Van Bourgondien, M. E., Wellman, G. J., & Love, S. R. The Childhood Autism Rating Scale (2nd ed.) (CARS2). (Los Angeles, CA: Western Psychological Services, 2010).
54. Sparrow, S. S., Cicchetti, D. V., Saulnier, C. A. Vineland Adaptive Behavior Scales. (Pearson, San Antonio, TX, ed. Third, 2016).
55. Ozonoff, S., Heung, K., Byrd, R., Hansen, R. & Hertz-Picciotto, I. The onset of autism: patterns of symptom emergence in the first years of life. *Autism Res* **1**, 320–328 (2008).
56. Sasson, N. J. et al. The broad autism phenotype questionnaire: prevalence and diagnostic classification. *Autism Res* **6**, 134–143 (2013).
57. Anderson, C. A. et al. Data quality control in genetic case-control association studies. *Nat. Protoc.* **5**, 1564–1573 (2010).
58. Chang, C. C. et al. Second-generation PLINK: rising to the challenge of larger and richer datasets. *Gigascience* **4**, 7 (2015).
59. Chiara, M. et al. CoVaCS: a consensus variant calling system. *BMC Genom.* **19**, 120 (2018).
60. Regier, A. A. et al. Functional equivalence of genome sequencing analysis pipelines enables harmonized variant calling across human genetics projects. *Nat. Commun.* **9**, 8 (2018).
61. Heng, L. Aligning sequence reads, clone sequences and assembly contigs with BWA-MEM. (arXiv:1303.3997v2 [q-bio.GN], 2013).
62. DePristo, M. A. et al. A framework for variation discovery and genotyping using next-generation DNA sequencing data. *Nat. Genet.* **43**, 491–498 (2011).
63. Wang, K., Li, M. & Hakonarson, H. ANNOVAR: functional annotation of genetic variants from high-throughput sequencing data. *Nucleic Acids Res* **38**, e164 (2010).
64. Robinson, J. T. et al. Integrative genomics viewer. *Nat. Biotechnol.* **29**, 24–26 (2011).
65. Choi, S. W., Mak, T. S.-H. & O'Reilly, P. F. Tutorial: a guide to performing polygenic risk score analyses. *Nat. Protoc.* **15**, 2759–2772 (2020).
66. Bacchelli, E. et al. An integrated analysis of rare CNV and exome variation in Autism Spectrum Disorder using the Infinium PsychArray. *Sci. Rep.* **10**, 3198 (2020).
67. Wang, K. et al. PennCNV: an integrated hidden Markov model designed for high-resolution copy number variation detection in whole-genome SNP genotyping data. *Genome. Res.* **17**, 1665–1674 (2007).
68. Colella, S. et al. QuantiSNP: an Objective Bayes Hidden-Markov Model to detect and accurately map copy number variation using SNP genotyping data. *Nucleic Acids Res* **35**, 2013–2025 (2007).
69. Douard, E. et al. Effect Sizes of Deletions and Duplications on Autism Risk Across the Genome. *Am. J. Psychiatry* **178**, 87–98 (2021).
70. Zarrei, M., MacDonald, J. R., Merico, D. & Scherer, S. W. A copy number variation map of the human genome. *Nat. Rev. Genet.* **16**, 172–183 (2015).
71. Roller, E., Ivakhno, S., Lee, S., Royce, T. & Tanner, S. Canvas: versatile and scalable detection of copy number variants. *Bioinformatics* **32**, 2375–2377 (2016).

Acknowledgements

We are extremely grateful to all the families who have participated in this study. We thank Evan E Eichler for collaboration on WGS. This research was funded by Italian Ministry of Health, grant number GR-2013-02357561; this work was also supported by #NEXTGENERATIONEU (NGEU) and funded by the Ministry of University and Research (MUR), National Recovery and Resilience Plan (NRRP), project MNESYS (PE0000006) – A Multiscale integrated approach to the study of the nervous system in health and disease (DN. 1553 11.10.2022) and project National Center for Gene Therapy and Drugbased on RNA Technology” (CN00000041) (M4C2 – Action 1.4- Call “Potenziamento strutture di ricerca e di campioni nazionali di R&S” (CUP J33C22001140001)). WGS data were generated at the New York Genome Center with funds provided by NHGRI Grant 3UM1HG008901. The Centers for Common Disease Genomics are funded by the National Human Genome Research Institute and the National Heart, Lung, and Blood Institute and the GSP Coordinating Center (U24HG008956) contributed to cross-program scientific initiatives and provided logistical and general study coordination. The funders played no role in study design, data collection, analysis and interpretation of data, or the writing of this manuscript.

Author contributions

Conceptualization: E.B., E.M.; Data curation: M.V., C.C., D.G., L.C., M.C.Z.; Formal analysis: M.V., F.C., L.S., E.B.; Funding acquisition: M.J.R., A.M., E.M., E.B.; Investigation: M.V., F.C., P.V., A.P., M.C.S., L.S., I.B., C.C., A.M., A.V., D.G., L.C., V.C., M.C.Z., E.B., E.M.; Methodology: F.C., E.B.; Resources: P.V., A.P., M.C.S., M.J.R., A.V.; Software: I.B.; Supervision: E.B., E.M.; Visualization: M.V., L.S., F.C., E.B.; Writing-original draft: F.C., E.B.; Writing-review & editing: M.V., F.C., P.V., A.P., M.C.S., A.V., E.B., E.M. All authors approved the submission of this manuscript. M.V. and F.C. contributed equally to this work.

Competing interests

MCZ declares to be a shareholder in Abbott, Abbvie, BMS, Merck, Pfizer, Thermo Fisher, and J&J.

Additional information

Supplementary information The online version contains supplementary material available at <https://doi.org/10.1038/s41525-024-00411-1>.

Correspondence and requests for materials should be addressed to Elena Maestrini or Elena Bacchelli.

Reprints and permissions information is available at <http://www.nature.com/reprints>

Publisher's note Springer Nature remains neutral with regard to jurisdictional claims in published maps and institutional affiliations.

Open Access This article is licensed under a Creative Commons Attribution 4.0 International License, which permits use, sharing, adaptation, distribution and reproduction in any medium or format, as long as you give appropriate credit to the original author(s) and the source, provide a link to the Creative Commons licence, and indicate if changes were made. The images or other third party material in this article are included in the article's Creative Commons licence, unless indicated otherwise in a credit line to the material. If material is not included in the article's Creative Commons licence and your intended use is not permitted by statutory regulation or exceeds the permitted use, you will need to obtain permission directly from the copyright holder. To view a copy of this licence, visit <http://creativecommons.org/licenses/by/4.0/>.

© The Author(s) 2024